

A Complementary Filter for Attitude Estimation of a Fixed-Wing UAV

Mark Euston, Paul Coote, Robert Mahony, Jonghyuk Kim and Tarek Hamel

Abstract—This paper considers the question of using a nonlinear complementary filter for attitude estimation of fixed-wing unmanned aerial vehicle (UAV) given only measurements from a low-cost inertial measurement unit. A nonlinear complementary filter is proposed that combines accelerometer output for low frequency attitude estimation with integrated gyrometer output for high frequency estimation. The raw accelerometer output includes a component corresponding to airframe acceleration, occurring primarily when the aircraft turns, as well as the gravitational acceleration that is required for the filter. The airframe acceleration is estimated using a simple centripetal force model (based on additional airspeed measurements), augmented by a first order dynamic model for angle-of-attack, and used to obtain estimates of the gravitational direction independent of the airplane manoeuvres. Experimental results are provided on a real-world data set and the performance of the filter is evaluated against the output from a full GPS/INS that was available for the data set.

I. INTRODUCTION

Attitude determination is an essential task for an Unmanned Aerial Vehicle (UAV). With the growing range of applications in UAV's, and the push to make vehicles cheaper and more reliable, it is of interest to develop robust and simple algorithms for attitude estimation [1], [9]. There is a large literature on attitude filtering techniques, see for example the recent review article by Crassidis *et al.* [6]. Most of the advanced filter techniques (particle filtering, etc.) are computationally demanding and unsuitable for the small scale embedded processors in UAV avionics systems. The two methods that are commonly employed are extended Kalman filtering (EKF) or some form of constant gain state observer, often termed a complimentary filter due to its frequency filtering properties for linear systems [12]. Extended Kalman Filtering has been studied for a range of aerospace applications [7], [9], [6], [16]. Such filters, however, have proved difficult to apply robustly [14], [4], [16]. In practice, many applications use simple linear single-input single-output complementary filters [16], [5]. In recent work, a number of authors have developed nonlinear analogous of single-input single-output (SISO) filters for attitude estimation [15], [19], [18], [13], [11], [2]. To implement these schemes on a UAV using inertial measurement unit (IMU) data the accelerometer output is used to estimate the gravitational direction. The recent work by the authors [8], [12] allows the full estimation of vehicle attitude (up to a constant heading error) as well as gyro biases using only accelerometer and gyrometer data. The filter fails, however,

when the vehicle dynamics are sufficiently important to prevent the accelerometer output providing a stable low-pass estimate of the gravitational direction. This is particularly the case for a fixed wing UAV manoeuvring in a limited space and making repeated rapid turns.

In this paper, we develop a nonlinear complementary filter, augmented by a simple first order model of vehicle dynamics that provides attitude estimates for a fixed wing UAV. The key contribution is to develop a model of the non-inertial acceleration of the airframe that can be used to compensate the accelerometer output to obtain a zero bias estimate of the gravitational direction. The model is based on a simple centripetal force model derived from the airspeed and the rate of turn of the vehicle. However, the angle-of-attack of the airplane is significantly higher during a sharp turn, and this must be modelled to correctly align the compensation terms for the accelerometer output. We address this problem by incorporating a simple first order model of the angle-of-attack dynamics of the airframe driven by the pitch rate measurement obtained from the gyrometer output. Gyrometer bias is estimated on-line by including an integral term into the complementary gain analogous to the process developed in earlier work [8], [12]. The combined system is simple to implement and achieves excellent performance, given the minimal data that is available. The algorithm is verified on experimental data from a fixed wing aerial robotic vehicle. The performance of the algorithm is confirmed by comparison with an attitude estimate obtained from a full INS/GPS stochastic filter that has been run on the experimental data. The algorithm is suitable for implementation on embedded computing systems characteristic of the avionics of mini-UAV platforms and with low-cost MEMS technology inertial sensors.

II. EXPLICIT COMPLEMENTARY FILTER

A complementary filter for attitude estimation performs low-pass filtering on a low-frequency attitude estimate, obtained from accelerometer data, and high-pass filtering on a biased high-frequency attitude estimate, obtained by direct integration of gyrometer output, and fuses these estimates together to obtain an all-pass estimate of attitude. When the pitch and roll of a airplane are modelled as decoupled processes, a SISO filter can be designed for each signal that uses the angle between the accelerometer output and the body-fixed-frame as attitude reference and the separate gyrometer axis output as velocity reference in a classical linear complementary filter [3]. When a low pass estimate of the full attitude can be reconstructed from the IMU measurements, for example if magnetometer data is also available and the full coupled rotation matrix for attitude

M. Euston, P. Coote, J. Kim and R. Mahony are with Department of Engineering, Australian National University, ACT, 0200, Australia. e-mail: firstname.surname@anu.edu.au.

T. Hamel is with I3S-CNRS, Nice-Sophia Antipolis, France. e-mail: thamel@i3s.unice.fr.

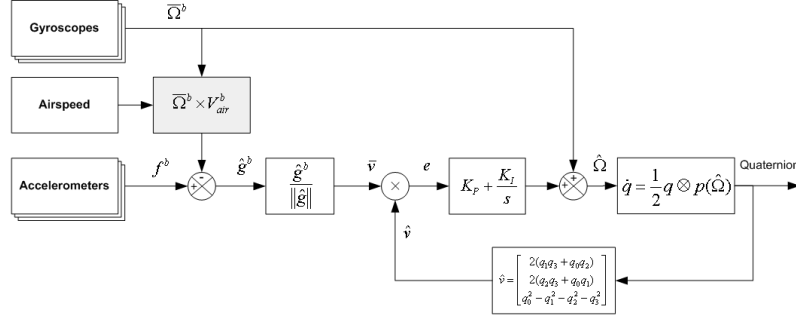


Fig. 1. Explicit Complementary Filter with acceleration compensation using airspeed data

can be computed as an algebraic function of the gravitational and magnetic fields measured in the body-fixed-frame, then nonlinear extensions of the complementary filters have been available for fifteen years [15], [18]. Magnetometers are rarely useful on small scale UAVs due to the perturbation of the magnetic field resulting from electric propulsion systems and other disturbances. The recent work by the authors [8], [12] provided a formulation of explicit complementary filtering (ECF), posed directly on the set of rotation matrices, that is driven by a single inertial direction measurement, such as provided by the accelerometer output, along with the gyrometer output.

The implementation of the explicit complementary filter is shown in Figure 1. The ECF uses a measurement of an inertial direction, denoted \bar{v} , along with the measured angular velocities $\bar{\Omega}$. In the case considered in this paper the inertial direction \bar{v} is derived from the best estimate of the gravitation direction g obtained from the system

$$\bar{v} = \frac{\hat{g}^b}{\|\hat{g}^b\|}. \quad (1)$$

The ECF can be expressed as an observer in quaternion form

$$\dot{\hat{q}} = \frac{1}{2} \hat{q} \otimes \mathbf{p}(\bar{\Omega} + \delta), \quad (2a)$$

$$\delta = k_P e + k_I \int e, \quad (2b)$$

$$e = \bar{v} \times \hat{v}, \quad (2c)$$

where \hat{q} is an estimate of the system attitude expressed as a unit quaternion. Here δ is an innovation in the filter equation generated by a proportional-integral block, and the error e is the relative rotation between the measured inertial direction \bar{v} and the predicted direction \hat{v} . The gains k_P and k_I are proportional and integral gains respectively, while $\mathbf{p}(\cdot)$ is the pure quaternion operator, $\mathbf{p}(\Omega) = (0, \Omega)$.

The estimate \hat{v} is the ECF's best estimate of the gravitational direction, that we take as being coincident with the Z-axis of the inertial frame. Thus, given the quaternion estimate \hat{q} one has

$$\hat{v} = \begin{bmatrix} 2(\hat{q}_1\hat{q}_3 + \hat{q}_0\hat{q}_2) \\ 2(\hat{q}_2\hat{q}_3 + \hat{q}_0\hat{q}_1) \\ \hat{q}_0^2 - \hat{q}_1^2 - \hat{q}_2^2 - \hat{q}_3^2 \end{bmatrix} \quad (3)$$

The ECF is most commonly used with proportional or proportional-integral (PI) compensation. The proportional term governs the frequency cross-over between accelerometer based attitude estimates and integrated gyro estimates. The integral term in the PI compensation corrects for gyro bias.

III. ATTITUDE MEASUREMENT WITH AN IMU

A six axis IMU provides measurements of angular velocity and acceleration. Typical units also provide a measurement of magnetic field, however, this is rarely a useful signal in a UAV application where the magnetic field is locally disturbed by the electrical subsystems of the vehicle.

The gyrometer measurements are modelled by

$$\bar{\Omega} = \Omega + b + \eta \quad (4)$$

where Ω is the true value, b is a slowly time-varying bias and η is a zero mean noise process. The angular rate can be integrated to maintain an estimate of the UAV's attitude, however, the bias and noise are also integrated resulting in the estimate diverging over time.

The accelerometers measure the *specific acceleration* in the Body-Fixed Frame (BFF),

$$f^b = a^b - g^b \quad (5)$$

where a^b is the acceleration of the UAV with respect to the inertial frame expressed in the BFF, and g^b is the gravitational acceleration expressed in the BFF. In level flight $a^b \approx 0$, therefore the gravity estimate, $\hat{g}^b = -f^b$, can be used as an input to the complementary filter 1. In this case, raw estimates of the roll ϕ and pitch θ [20] can be computed directly from the \bar{v}

$$\hat{\phi}_f = \text{Atan2}(-f_y, -f_z) \quad (6)$$

$$\hat{\theta}_f = \text{Atan2}(f_x, \sqrt{f_y^2 + f_z^2}). \quad (7)$$

These estimates are used directly in the implementation of SISO complementary filters [16], [5]. When the aircraft is manoeuvring $a^b \neq 0$ and the above construction is not valid.

A. Acceleration Compensation Using Airspeed Data

A simple dynamic model is proposed to estimate the acceleration of the UAV during sustained turns based on gyrometer and airspeed data. We assume the aircraft turns with a constant turn radius $\rho > 0$, which (excluding the entry and exit of the turn) is approximately the case for an aircraft performing a level turn with constant airspeed.

In a flat turn with constant radius the non-zero component of the acceleration, experienced by the vehicle, is the centripetal acceleration

$$\hat{a} = \Omega \times (\Omega \times \rho \mathbf{r}) \quad (8)$$

where Ω is the angular rate and ρ is the turn radius and \mathbf{r} is the unit vector from the airplane to the centre of the turn.

In stationary air, the linear velocity of the vehicle during a flat turn is given by $\Omega \times \rho \mathbf{r}$. Almost always, there will be a non-zero wind disturbance, however, this can be approximated as a constant velocity wind with additional gust disturbances. The gust disturbances are considered as a zero bias noisy disturbance, while constant wind velocity is dealt with by choosing the inertial frame to move with constant mean wind velocity. Thus, with respect to the (moving) inertial frame the wind has zero mean velocity. Since we are only interested in attitude estimation in this paper, and none of the measurement devices depend on position of the vehicle, this assumption preserves the structure of the explicit complementary filter. It follows that one can approximate $\Omega \times \rho \mathbf{r}$ by the vehicle airspeed V_{air} to cancel dependence on the unknown turn geometry

$$\hat{a} = \Omega \times V_{\text{air}} \quad (9)$$

The magnitude $|V_{\text{air}}|$ of the airspeed can be measured from calibrated dynamic pressure measurements and relates to airspeed not ground speed. If GPS measurements were filtered to obtain velocity estimates then the overall attitude observer would need to be augmented with an estimator to identify the mean wind velocity, an added complexity in the filter design. Conversely, in the approach taken in this paper, the mean wind velocity does not need to be estimated, however, only the magnitude $|V_{\text{air}}|$ can be directly measured and it is necessary to separately estimate the vector direction of V_{air} .

The angle-of-attack of an aircraft is the angle between the chord line of an airfoil and the vector representing the relative motion between the airfoil and the air. As the angle-of-attack increases, for constant airspeed, the relative lift of the airfoil increases. When an airplane turns, the additional centripetal acceleration is provided by increased angle-of-attack. To ensure that additional acceleration is correctly aligned for the turn, the airplane banks or rolls into the turn. In a balanced turn, the increased lift from the airfoil is inclined with respect to the vertical and decomposes into a vertical and horizontal component. In order for the airplane to maintain altitude the vertical component of the lift must continue to cancel gravity and this determines the required increase in angle-of-attack. The resulting horizontal acceleration is the centripetal acceleration and determines the rate of turn, depending on the vehicle airspeed. During a turn,

the acceleration remains constant with respect to the body-fixed-frame. Such trajectories are termed trim trajectories and, apart from short transients, are the normal flight regime for aircraft not engaged in acrobatics.

Based on the above discussion, a reasonable model of an aircraft in a turn is to assume zero sideslip but changing angle-of-attack. That is we model

$$V_{\text{air}} = |V_{\text{air}}| \begin{pmatrix} \cos(\alpha) \\ 0 \\ \sin(\alpha) \end{pmatrix} \quad (10)$$

where α is the changing angle of attack.

The final component of modelling the turn dynamics is to incorporate a dynamic model for the angle-of-attack α . Since only the angle-of-attack of the vehicle is of interest then we use equations of motion for the longitudinal motion of an aircraft [17, pg. 115]. From these equations it is only necessary to consider the dynamics of the angle-of-attack, and furthermore since no extreme manoeuvres will be undertaken, a linearised version of these dynamics will suffice

$$\dot{\alpha} = -\frac{c_0}{|V_{\text{air}}|} \alpha + \dot{\theta} + \alpha_0 \quad (11)$$

where c_0 and α_0 are constants. The constant c_0 is a time constant depending on the thrust force of the vehicle and α_0 is a constant set-point that encodes the static angle-of-attack required to sustain level flight. The pitch rate $\dot{\theta} = \langle e_2, \Omega \rangle$ is the rate of rotation around the e_2 BFF axis. During a balanced turn, the pitch rate will be a constant value as the plane continually pitches up, since it is banked over, to rotate around the radius of the turn. Thus, the angle-of-attack during a turn will be offset from the set-point α_0 . The moment that the turn is ended, the angle-of-attack will settle back to the set-point with time-constant $c_0/|V_{\text{air}}|$.

Remark: In the proposed design, the constants c_0 and α_0 must be known *a-priori*. This is discussed further in the experimental results.

Once the angle-of-attack is computed using (11) the vectorial airspeed can be computed using (10). These values in turn lead to an estimate of \hat{a} using (9). This estimate is naturally expressed in the body-fixed-frame \hat{a}^b . Given the actual output from the accelerometers f^b the estimate of the gravitational direction is given by

$$\hat{g}^b = -(f^b - \hat{a}^b). \quad (12)$$

The estimated gravitational direction is then used in (1) to determine the vectorial measurement used in the complementary filter implementation. The full block diagram of the resulting filter is shown in Figure 1 excluding the additional dynamics for the angle-of-attack.

IV. EXPERIMENTAL RESULTS

The filter was tested on flight data obtained from a fixed wing UAV from the Australian Centre for Field Robotics, University of Sydney. The UAV flew the circuit shown in Figure 2 at approximately 36m.s^{-1} with relatively constant altitude. The UAV flies anti-clockwise several times and does one figure-of-eight. A GPS/INS Kalman Filter has previously

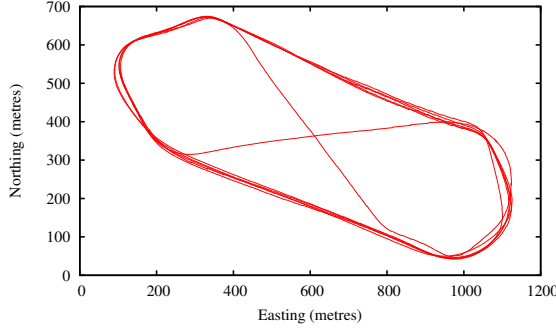


Fig. 2. Flight Path for experimental data set

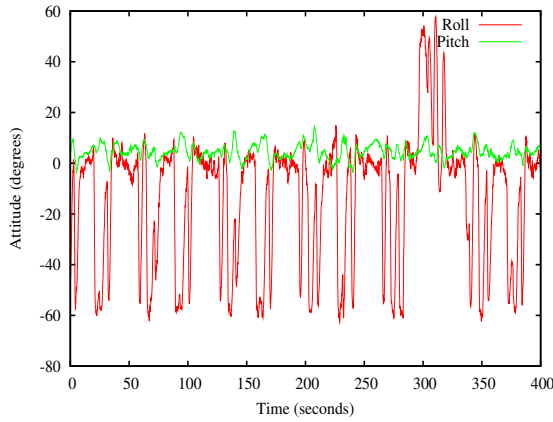


Fig. 3. Attitude estimates for experimental data obtained using GPS/INS Kalman filter [10]

been tested on this data set [10], that was used as our best estimate of the true attitude (Figure 3).

To implement the proposed filter it is necessary to derive a model of the longitudinal dynamics of the vehicle. In particular, the values of constants c_0 and α_0 in (11) must be known. System identification for the experimental data was undertaken using the interactive systems identification toolbox in MATLAB. The values used in the following experiments were

$$c_0 = 72 \text{m.rad.s}^{-1}, \quad \alpha_0 = 0.2 \text{rad}.$$

In the model identification we assume that the vehicle velocity is constant at $V_{\text{air}} = 36 \text{m.s}^{-1}$ to enable us to use linear systems identification tool. The longitudinal dynamics of the angle-of-attack were modelled by

$$\frac{d}{dt}\alpha = -2\alpha + \dot{\theta} + 0.2.$$

Note that the airspeed is not assumed constant in the calculation of centripetal acceleration (9).

A. Acceleration Compensation

To evaluate the performance of the acceleration compensation, we compare the unfiltered attitude obtained from the

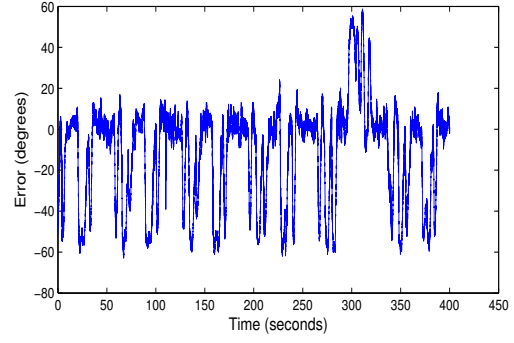


Fig. 4. Roll error from raw roll estimates obtained from the accelerometer readings without compensation. The large deviations of the error correspond to the raw roll estimates failing to detect the banking manoeuvres of the airplane.

TABLE I
PITCH ERROR STATISTICS FOR DIRECT ATTITUDE RECONSTRUCTION
(LOW-PASS FILTERED)

	Average	Std. Dev.
$\hat{a} = 0$	-2.2336	4.7455
$\hat{a} = \Omega \times \hat{V}_{\text{air}}$	0.583	6.7533

gravity estimate to the attitude estimate of the GPS/INS filter (Figure 3). The roll and pitch for the unfiltered gravity estimate are computed by substituting the estimate \hat{g} into the equations for pitch (7) and roll (6)

$$\hat{\phi}_f = \text{Atan2}(-(f_y - \hat{a}_y), -(f_z - \hat{a}_z)) \quad (13)$$

$$\hat{\theta}_f = \text{Atan2}(f_x - \hat{a}_x, \sqrt{(f_y - \hat{a}_y)^2 + (f_z - \hat{a}_z)^2}) \quad (14)$$

where $\hat{a} = \Omega \times \hat{V}_{\text{air}}$. The actual raw data is heavily corrupted by high frequency noise from engine vibration and the plots shown have been low pass filtered (with roll off at 25rad.s^{-1}) to show the low-frequency structure that is relevant to the filter response. Figure 4 shows the error between the GPS/INS solution and the raw estimate of the airplane roll derived from the accelerometer measurements, i.e. using f^b directly in (6). It is clear that the raw accelerometer output fails to detect the banking turns of the vehicle. Figure 5 shows the histogram of the error. The multi-modal nature of the error shows clearly, with the main mode in the distribution corresponding to normal flight and the secondary modes on either side corresponding to banking turns, primarily to the left, but also a smaller mode to the right from when the airplane undertook a figure-of-eight manoeuvre. Figure 6 shows the error between the GPS/INS solution and the compensated estimate of the airplane roll derived from the accelerometer measurements adjusted for centripetal acceleration with the angle-of-attack model incorporated (13). Adjusting for the centripetal acceleration clearly overcomes the major error in the low-frequency attitude data. It is clear, however, that the accelerometer data remains highly corrupted by engine vibration.

To provide a quantifiable measure of improvement we

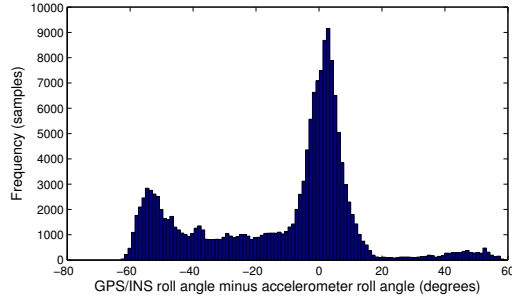


Fig. 5. Histogram of unfiltered and uncompensated roll errors showing the effect of centripetal force on accelerometers during banked turns as two side modes on the main distribution

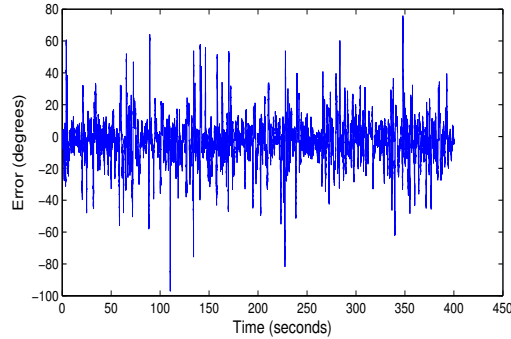


Fig. 6. Roll error from compensated roll estimates obtained from the accelerometer readings adjusted for centripetal acceleration.

have computed the average and the standard deviation of the roll and pitch error. The average error should ideally be zero — non-zero average error indicates a low frequency error which will degrade filter performance. In practice, the GPS/INS data is itself noisy, and subject to disturbances from external data sources (GPS) that are not available to the ECF. Consequently, it is expected that there will be a residual error. Tables I and II indicate that incorporating the angle-of-attack dynamic model reduces the pitch and roll errors by 70% and 60% respectively.

B. Filter Performance

The data was passed through an explicit complementary filter. Results were obtained both for the augmented filter, with dynamic angle-of-attack model, and for the case where the uncompensated gravity estimate was used. Note that the compensated data was passed directly into the ECF and was not low-pass pre-filtered.

TABLE II
ROLL ERROR STATISTICS FOR DIRECT ATTITUDE RECONSTRUCTION
(LOW-PASS FILTERED)

	Average	Std. Dev.
$\hat{a} = 0$	-11.4464	24.8136
$\hat{a} = \Omega \times \hat{V}_{\text{air}}$	-2.8277	13.8126

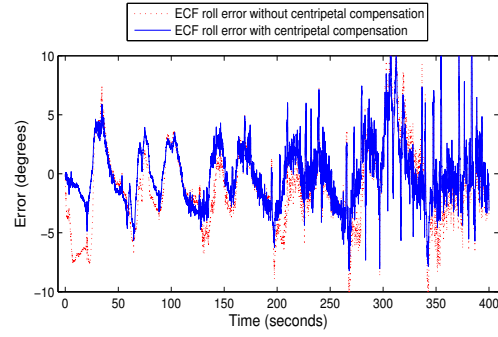


Fig. 7. Error between the ECF and ECF- \hat{a} filters and the full GPS/INS solution.

TABLE III
ECF AND ECF- \hat{a} PITCH ERROR STATISTICS

	Average	Std. Dev.
$\hat{a} = 0$	-8.4887	3.725
$\hat{a} = \Omega \times \hat{V}_{\text{air}}$	-1.3531	1.645

The filter block $C(s)$ in the complementary filter contains two gains K_P and K_I

$$C(s) = K_P + \frac{K_I}{s}.$$

The complementary filter fuses estimates with low frequency validity of the attitude (expressed as the gravitational direction estimate), and provides a low pass filtering of these estimates that rolls off at $K_P \text{ rad.s}^{-1}$, with an attitude estimate provided by integrated gyrometer output that has high frequency validity, and provides a high pass filtering of these estimates that rolls on at frequency $K_P \text{ rad.s}^{-1}$. For the data considered a gain of $k_P = 0.04 \text{ rad.s}^{-1}$ was chosen as the cross-over frequency. The low value of the proportional gain is associated with the high level of engine vibration noise in the accelerometer data and the necessity to filter this vibration from the output. The gain K_I is associated with the bias estimation process of the complementary filter. Typically, this gain is chosen a factor of 10 to 100 times slower than the proportional gain in order to help decouple the interaction of the main filter and bias dynamics. In this case the associated rise time of the bias estimate is in the order of 5-10 minutes. This is a reasonable estimate for bias estimation in a fixed wing UAV application where mission lengths are often hours long and bias variation is depends on slowly changing mission conditions. The data set considered is only 400s long. For such a short data set the slow dynamics associated with the bias estimate are not active. Consequently, in the experimental studies undertaken on this data set the bias gain $K_I = 0$ is set to zero. On a longer data set a value of 0.002 rad.s^{-1} would be a suitable choice.

For the explicit complementary filter, the filtered estimate of the gyrometer output should be used in the computation

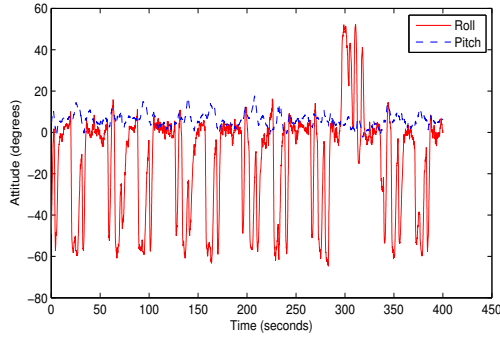


Fig. 8. The output of the ECF- \hat{a} filter. This plot can be compared with Figure 3.

TABLE IV
ECF AND ECF- \hat{a} ROLL ERROR STATISTICS

	Average	Std. Dev.
$\hat{a} = 0$	-1.0318	3.4989
$\hat{a} = \Omega \times \hat{V}_{\text{air}}$	-0.0136	2.7099

of the centripetal acceleration

$$\hat{a} = \hat{\Omega} \times \hat{V}_{\text{air}}$$

where $\hat{\Omega} = \bar{\Omega} + \delta$ is the driving term in (2a) in the complementary filter (2). The innovation term δ acts to remove low frequency noise, and in particular removes bias terms from the direct measurement $\bar{\Omega}$ of the angular velocity.

Figure 7 shows the relative performance of the roll estimate for the explicit complimentary filter based both on raw accelerometer attitude computations (ECF) and on the explicit complementary filter with adjustment for centripetal acceleration incorporating the angle-of-attack model (ECF- \hat{a}). It is interesting that there is less difference between these two traces as may be expected based on Figures 4 and 6. This is due to the low value of K_P chosen, itself a consequence of the very large amounts of engine noise present in the accelerometer data. The statistical performance of the filters is compared in Tables III and IV. Here, the advantages of the ECF- \hat{a} filter is clear with pitch error decreased by 85% and roll error decreased by 99% with inclusion of the angle-of-attack model. Figure 8 shows the actual output of the ECF- \hat{a} filter in the same format as Figure 3. Given the limited data resources of the ECF- \hat{a} (IMU, dynamic pressure) and its simple structure, the filter performance is highly satisfactory.

V. CONCLUSION AND FURTHER WORK

The Explicit Complementary Filter (ECF) was extended to incorporate a model of the longitudinal angle-of-attack dynamics of a fixed-wing aircraft. With this model, the ECF- \hat{a} , using only IMU and dynamics pressure measurements achieved attitude filtering performance of the same quality as a full extended Kalman filter that exploited full GPS/INS data. The ECF shows significant potential as a simple and robust attitude filter for small scale UAV vehicles.

VI. ACKNOWLEDGMENTS

The authors wish to thank the Australian Centre for Field Robotics, University of Sydney, for the flight data used in this paper.

REFERENCES

- [1] A-J. Baerveldt and R. Klang. A low-cost and low-weight attitude estimation system for an autonomous helicopter. *Intelligent Engineering Systems*, 1997.
- [2] S. Bonnabel, P. Martin, and P. Rouchon. A non-linear symmetry-preserving observer for velocity-aided inertial navigation. In *American Control Conference, Proceedings of the*, pages 2910–2914, June 2006.
- [3] G. Buskey, J. Roberts, P. Corke, P. Ridley, and G. Wyeth. Sensing and control for a small-size helicopter. In *Experimental Robotics VIII: Springer Tracts in Advanced Robotics*, volume 5. Springer, February 2004.
- [4] D. Choukroun, I.Y. Bar-Itzhack, and Y. Oshman. Novel quaternion kalman filter. *IEEE Transactions on Aerospace and Electronic Systems*, 42(1):174–190, January 2006.
- [5] P. Corke. An inertial and visual sensing system for a small autonomous helicopter. *J. Robotic Systems*, 21(2):43–51, February 2004.
- [6] John L. Crassidis, F. Landis Markley, and Yang Cheng. Nonlinear attitude filtering methods. *Journal of Guidance, Control, and Dynamics*, 30(1):12–28, January 2007.
- [7] D. Gebre-Egziabher, R.C. Hayward, and J.D. Powell. Design of multi-sensor attitude determination systems. *IEEE Transactions on Aerospace and Electronic Systems*, 40(2):627–649, April 2004.
- [8] T. Hamel and R. Mahony. Attitude estimation on $SO(3)$ based on direct inertial measurements. In *Robotics and Automation, 2006. ICRA 2006. Proceedings 2006 IEEE International Conference on*, pages 2170–2175, Orlando FL, USA, April 2006. Institute of Electrical and Electronic Engineers.
- [9] M. Jun, S. Roumeliotis, and G. Sukhatme. State estimation of an autonomous helicopter using Kalman filtering. In *Proc. 1999 IEEE/RSJ International Conference on Robots and Systems (IROS 99)*, 1999.
- [10] J. Kim. *Autonomous Navigation for Airborne Applications*. PhD thesis, Australian Centre for Field Robotics, The University of Sydney, 2004.
- [11] R. Mahony, T. Hamel, and Jean-Michel Pflimlin. Complementary filter design on the special orthogonal group $SO(3)$. In *Proceedings of the IEEE Conference on Decision and Control, CDC05*, Seville, Spain, December 2005. Institute of Electrical and Electronic Engineers.
- [12] Robert Mahony, Tarek Hamel, and Jean-Michel Pflimlin. Non-linear complementary filters on the special orthogonal group. *IEEE Transactions on Automatic Control*, to appear. Accepted for publication October 2007.
- [13] D.H.S. Maithripala, J.M. Berg, and W.P. Dayawansa. An intrinsic observer for a class of simple mechanical systems on a lie group. In *American Control Conference*, volume 2, pages 1546–1551, 30 June–2 July 2004.
- [14] J. M. Roberts, P. I. Corke, and G. Buskey. Low-cost flight control system for small autonomous helicopter. In *Australian Conference on Robotics and Automation, Auckland, 27–29 Novembre*, pages 71–76, 2002.
- [15] S. Salcudean. A globally convergent angular velocity observer for rigid body motion. *IEEE Transactions on Automatic Control*, 46, no 12:1493–1497, 1991.
- [16] S. Saripalli, J.M. Roberts, P.I. Corke, G. Buskey, and G.S. Sukhatme. A tale of two helicopters. In *Proceedings of the IEEE/RSJ International Conference on Intelligent Robots and Systems*, volume 1, pages 805–810, Las Vegas, 27–31 Oct. 2003.
- [17] B.L. Stevens and F.L. Lewis. *Aircraft Control and Simulation*. John Wiley and Sons, second edition, 2003. ISBN 0471371459.
- [18] J. Thienel and R. M. Sanner. A coupled nonlinear spacecraft attitude controller and observer with an unknown constant gyro bias and gyro noise. *IEEE Transactions on Automatic Control*, 48(11):2011 – 2015, Nov. 2003.
- [19] B. Vik and T. Fossen. A nonlinear observer for GPS and INS integration. In *Proceedings of the 40th IEEE Conference on Decision and Control*, 2001.
- [20] M. Wang, Y. Yang, R.R. Hatch, and Y. Zhang. Adaptive filter for a miniature mems based attitude and heading reference system. In *Position Location and Navigation Symposium*, pages 193–200, 26–29 April 2004.